Heat Transfer Enhancement in Ventilated Brake Disk Using Double Airfoil Vanes

A. Nejat[1]
Assistant Professor
e-mail: nejat@ut.ac.ir

M. Aslani
e-mail: m.aslani@ut.ac.ir

E. Mirzakhalili
e-mail: e.mirzakhalili@ut.ac.ir

R. Najian Asl
e-mail: r.najian@ut.ac.ir

School of Mechanical Engineering,
College of Engineering,
University of Tehran,
Tehran, Iran

The aim of this research is to enhance the heat transfer of ventilated brake disks using modified vanes. The investigated braking scenario is a hold braking deceleration during a downhill drive. A simple model for computing the steady state vane's temperature is presented. The heat transfer coefficient (HTC) of the brake disk's ventilation is estimated by means of a verified CFD computation. A novel design for the vanes is proposed using an airfoil profile to improve the air pumping efficiency increasing the flow velocity between vanes. For further improving the ventilating capacity, a secondary airfoil vane is introduced to the primary airfoil vane design. The computed results estimate 17% to 29% improvement in HTC number for new vane design at different disk's angular velocities. [DOI: 10.1115/1.4004931]

Keywords: disk brake ventilating, airfoil, thermal efficiency, CFD, HTC

1 Introduction

A braking system of a vehicle changes its kinetic energy to thermal energy in order to reduce the speed of the vehicle or to stop it completely. In this action, the generated heat is conducted to the components of the operating (brake) system. What is called the brake fade is the tragic result of this cyclic heating. This fade can be caused by thermal stresses, brake liquid vaporization (losing its hydraulic properties), appearance of hot spots, thermally excited vibration, bearing failure etc. For instance, Brake fluid vaporization has been suspected as a possible cause of some accidents particularly for passenger cars equipped with aluminum calipers and with a limited air flow to the wheel brake systems [1,2]. To minimize these malfunctions many solutions have been proposed depending on the type of the operating system (drum or disk brakes).

The brake disks (more commonly used than the drum brakes) utilize rubbing or friction surfaces to decelerate the ongoing car. The friction materials in the form of the brake pads (mounted on a device called the brake caliper) are forced mechanically, hydraulically, pneumatically, or electromagnetically against both sides of the disk. Providing a better ride quality by lowering the unsprung mass of the vehicle, brake disks weigh less than other braking systems. On the other hand they intrinsically can generate more braking power than other systems [3,4]. One layer solid disk Fig. 1(*a*) is the common type of braking disks; more than 90% of the generated energy is dissipated through disk. This major amount of the heat energy (About 666 kJ in a common highway stop which can bring about 2 liters of water to boil) diffuses through conduction within the disk and through the hub. This heat is then dissipated by convection and radiation from the outer surfaces of the disk and the hub flange. In high demand braking applications, vented disks consisting of two rubbing surfaces separated by radial vanes are normally employed because they utilize a greater surface area to dissipate the heat. The ventilated disks act like an air pump, circulating air from center (through the passages) to the outside of the rotor. Many geometry profiles are designed for the mean layer of the co-rotating disk in order to improve the aerodynamics cooling properties of the disk, thus, increasing the heat transfer coefficient (HTC). These geometries are shown in Fig. 1(*b*) including straight vanes, curved vanes, and pillar posts.

Beside a large number of patents presenting new geometries without a direct scientific claim, research studies in the literature are mainly focused on finding a true model for this complex thermal-fluid system. Limpert [5] compared the solid and the ventilated rotor thermal performance and concluded that the total convective heat transfer coefficient consisted of approximately one-third from the vanes, and two-thirds from the friction surfaces, exposed to the ambient air. He also noted that at higher rotor speeds the internal cooling may contribute as much as 50% or 60% to the total cooling. Also the temperature distribution of the solid rotors has been investigated by Limpert [4] by the assumption of a constant heat flux during constant-speed downhill braking. Sisson [6] used Duhamel's theorem to integrate an analytical slab solution with a nodal solution to come up with a general formula for the straight vanes. Wallis et al. [7] investigated different vane geometries and finally concluded that the total heat transfer from the straight round radial vane and pillar post passages perform up to 20% better than the straight vane rotor in heat dissipation. Also comparison of different rotors clearly demonstrated the importance of passage inlet design for ventilated rotors in this study. An analytical model was presented by Gao and Lin [8] for the determination of the contact temperature distribution on the working surface of a solid brake disk. It was also concluded that operating conditions of the brake essentially influence the surface temperature distribution and the maximal contact temperature. The particle image velocimetry (PIV) was used by Johnson et al. [9] to measure the air flow velocity through a high solidity radial fan utilized as an automotive vented brake rotor. They concluded that as a result of large flow separation regions in the internal vane-to-vane passages, (on the suction side surfaces) the overall heat transfer was reduced noticeably. Sakamoto [10] did some experimental and analytical investigation on ventilated brake disks and concluded that the heat convection area is more important than the thickness or number of fins; moreover, the air velocity through the fins plays an essential role here. Chi et al. [11] examined the effects of geometrical parameters of pillar post rotors on the thermal performance of the automotive vehicle brakes by using numerical methods. McPhee and Johnson [12] used experimental and analytical methods on the brake rotor to determine the phase-averaged velocity field of the flow in vanes using PIV. They concluded that the internal coefficient increased much more rapidly with increasing speed. This result illustrates the importance of vented rotors for operation at moderate speeds. Talati and Jalalifar [13] investigated the heat transfer in straight vanes of a passenger car front brake disk using finite element method. Same authors in Ref. [14] obtained the governing heat equations for the disk-pad system in form of transient heat equations in which heat generation is dependent on time and space.

[1]Corresponding author.

Contributed by the Heat Transfer Division of ASME for publication in the JOURNAL OF THERMAL SCIENCE AND ENGINEERING APPLICATIONS. Manuscript received May 4, 2011; final manuscript received August 15, 2011; published online November 7, 2011. Assoc. Editor: Zahid Ayub.

Copyright © 2011 by ASME

Downloaded From: http://thermalscienceapplication.asmedigitalcollection.asme.org/pdfaccess.ashx?url=/data/journals/jtsebv/28835/ on 02/06/2017 Terms of Use: http://www.asr

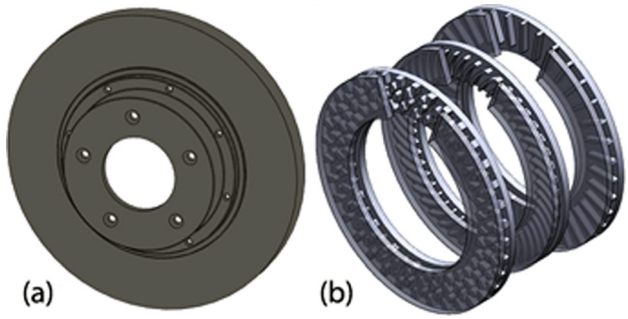

Fig. 1 Brake disks, (*a*) one layer solid disk and (*b*) types of ventilated brake disks

In this research, a novel design for the geometry of the vanes is presented by employing airfoils as the well known profiles to accelerate the air flow. Here the standard NACA airfoils, presented by the exact mathematical equation, are used as the working vanes of the rotating disk. Being familiar with the physics of the flow over these profiles, a superior shape and arrangement for vanes are suggested. The new design is numerically tested in brake disk cooling and its promising performance is compared with the classic straight vane design in some vehicle speeds. Increasing the speed of the air passed by vanes has been a general guide considered in almost all articles in the field, and we have taken the full advantage of this design guideline. Also another heat transfer improving factor, i.e., keeping the flow attached to the vanes, is explored in detail through computational fluid dynamics (CFD), simulations.

The Sec. 2 introduces the theory behind this study and describes the numerical model as well as the verification process. In Sec. 3, the design strategy is discussed in detail and finally the paper is come to the end by Sec. 4 highlighting the findings of the research work.

2 Theory and Modeling

2.1 Heat Transfer. The temperature rising of a brake disk in a braking operation depends on the mass and the velocity (i.e., the linear momentum) of the vehicle, the retardation rate and the braking event duration (deceleration rate). When the braking duration is short and the retardation is relatively mild, the rotor and the friction material normally absorb most of the generated thermal energy. In extreme braking operations such as steep descents or repeated high speed brake applications, the sufficient heat dissipation becomes critical to ensure reliable continued braking. The heat is dissipated by radiation, conduction, and convection. Radiation heat transfer from the rotor will have its greatest effect at higher temperatures but must be controlled to prevent beading of the tire. It is estimated that the amount of heat dissipation through radiation under typical braking conditions is negligible [5,13]. Therefore as many other studies in the literature, here, the radiation is neglected. Although conduction plays an important role in terms of heat transfer in the brake disk, it has adverse results in the nearby components as mentioned before. The third and the most important way to dissipate heat from the disks is convection. During a single stop nearly all of the braking energy is absorbed by the brake rotor; consequently only during repeated and continued braking the convective heat transfer coefficient does affect brake temperature [5]. Convection may happen in two ways, sides of the rotor and the vanes of a ventilated disk. Rate of heat transfer (W) by means of convection [4,12] can be expressed by the following general formula [15]

$$Q = Ah(T_s - T_\infty) \tag{1}$$

Here h refers to convection heat transfer coefficient $\mathrm{W/m^2\,K}$, A is surface area of the ventilation $(\mathrm{m^2})$, T_s is surface temperature of the vanes (K) and finally T_∞ is ambient air temperature (K). To increase the rate of heat dissipation, one should simply increase the ventilation area (A) or the convective heat transfer coefficient (h). The surface temperature T_s is not a design parameter and changes with time and finally the overall aim is to reduce it. Ventilation area is confined to the limited space available between two co-rotating disks. This might change slightly, depending on the type of the ventilation and the vanes geometry, but the overall effect is very slight and can be ignored when disks of the same diameters are compared. The most reasonable way to accomplish our goal, i.e., increasing the heat dissipation rate, is to improve the convective heat transfer coefficient. This parameter is highly dependent on the speed of the cooling airflow in the vanes of the ventilated brake disk [5,11,12]. In fact the airflow passing through the annular passages is directed by these vanes, and consequently their geometry (vane's geometry) determines the quality of disk cooling.

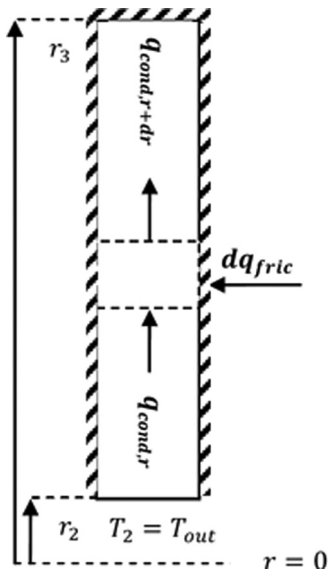

Fig. 2 Geometry and boundaries of the problem

2.2 Modeling. Before going through the modeling of a brake disk's ventilation, first the strategy of braking should be determined. Different strategies may be available depending on the driving situations, but as we want to assess the capacity of the brake disks in extreme braking operations, the steady state braking, which in terms is the easiest scenario of modeling, was chosen as the limit of the heat generation. This would happen for example in descending from a downhill. According to Ref. [16], a saturated (quasi-stationary) temperature distribution during repeated braking happens. This temperature can be obtained from a simple but effective heat transfer computation as following.

Table 1 Constants of the Eqs. (4) and (5)

Constant	Definition	Magnitude
μ	Friction coefficient	0.333
P	Applied pressure on disk	5 Mpa [2]
K	Thermal conduction coefficient	43.5 W/m K
T	Disk thickness	24 mm
Ω	Angular velocity	40∼100 rad/s
r_2	Inner radius	130 mm
r_3	Outer radius	180 mm

Downloaded From: http://thermalscienceapplication.asmedigitalcollection.asme.org/pdfaccess.ashx?url=/data/journals/jtsebv/28835/ on 02/06/2017 Terms of Use: http://www.asr

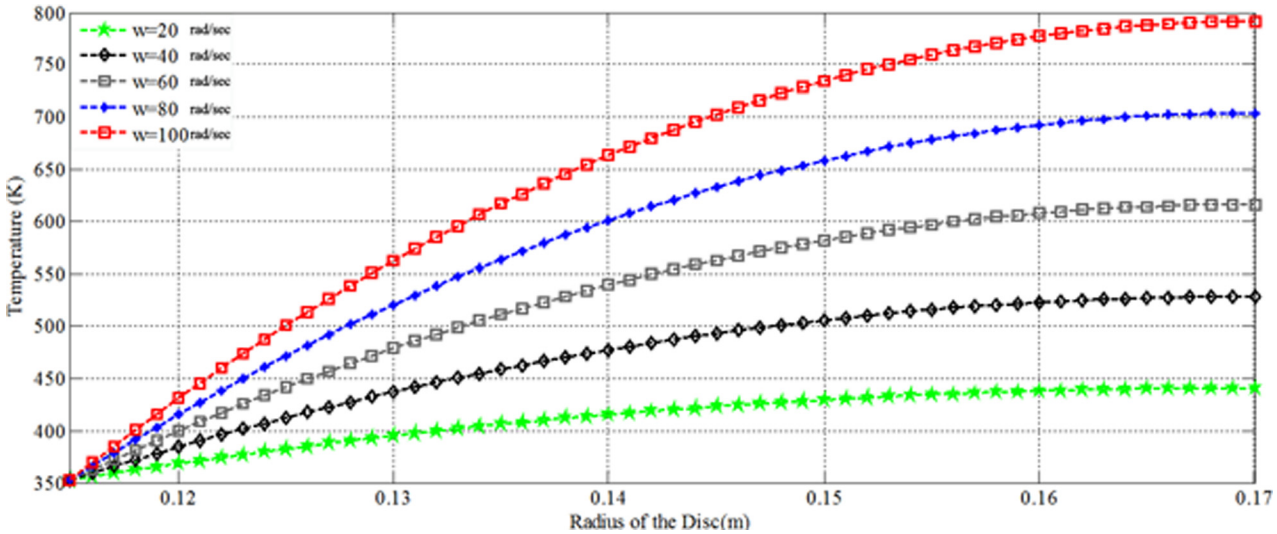

Fig. 3 Temperature field of an isolated brake disk

Table 2 Flow condition properties and simulation details

Meshing parameters	Mesh type	Unstructured triangles
	Number of control volumes	56,000-86,000
	Element size	2.75×10^{-4} to 2.627×10^{-3} m^2
Solver	Numerical discretization	2nd-order upwind
	Turbulence model	Realizable k-ϵ
Boundary Conditions	Disk inner hub	Pressure inlet
	Disk outer hub	Pressure outlet
	Vane's steady temperature	600 °C
Fluid and flow properties	Reynolds[a] ($\mathrm{Re} = \rho \mathrm{VL}/\mu$)	$2.46 \times 10^4 \sim 1.23 \times 10^5$
	Turbulent intensity	0.045
	Prandtl ($\mathrm{Pr} = \nu/\alpha$)	0.685

[a]L is the diameter of the disk and V is calculated for each angular velocity ($V = \mathrm{r}\omega$).

Considering an isolated brake disk (Fig. 2) rotating in an angular velocity ω, an analytical temperature field for the disk is obtained by assuming a differential element of the disk and solving an ordinary differential equation (ODE).

- Differentials

$$\mathrm{d}F_n = p.\mathrm{d}A = p(2\pi r)\mathrm{d}r;\ (\text{normal force}, \mathrm{N})$$

$$\mathrm{d}F_t = \mu.\mathrm{d}F_n = \mu.(p.\mathrm{d}A) = \mu p(2\pi r)\mathrm{d}r;\ (\text{tangential force}, \mathrm{N})$$

$$\mathrm{d}M = r.\mathrm{d}F_t = \mu p(2\pi r^2)\mathrm{d}r;\ (\text{torque}, \mathrm{N.m})$$

$$\mathrm{d}q_f\omega.\mathrm{d}M = 2\pi p\mu\omega r^2.\mathrm{d}r;\ (\text{generated heat}, \mathrm{W})$$

- Governing ODE

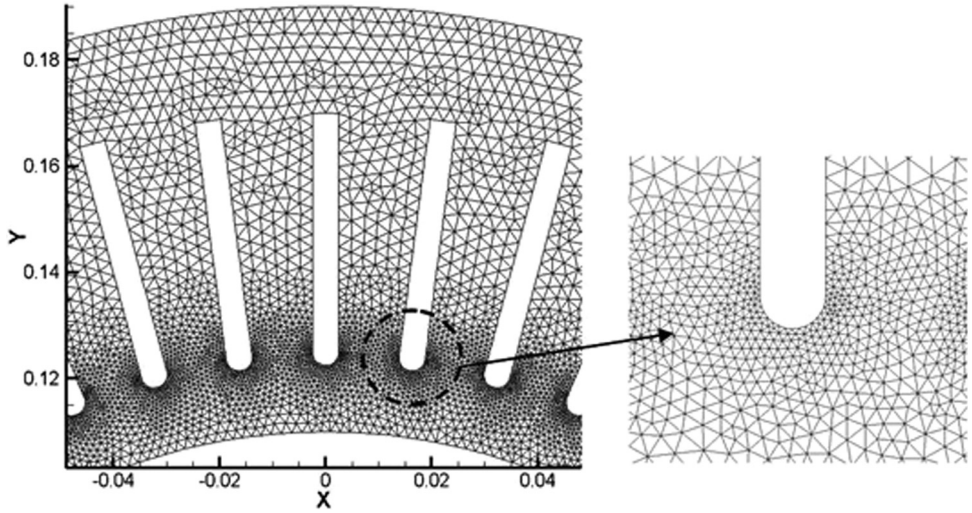

Fig. 4 Triangle meshing for a straight vane disk

Downloaded From: http://thermalscienceapplication.asmedigitalcollection.asme.org/pdfaccess.ashx?url=/data/journals/jtsebv/28835/ on 02/06/2017 Terms of Use: http://www.asr

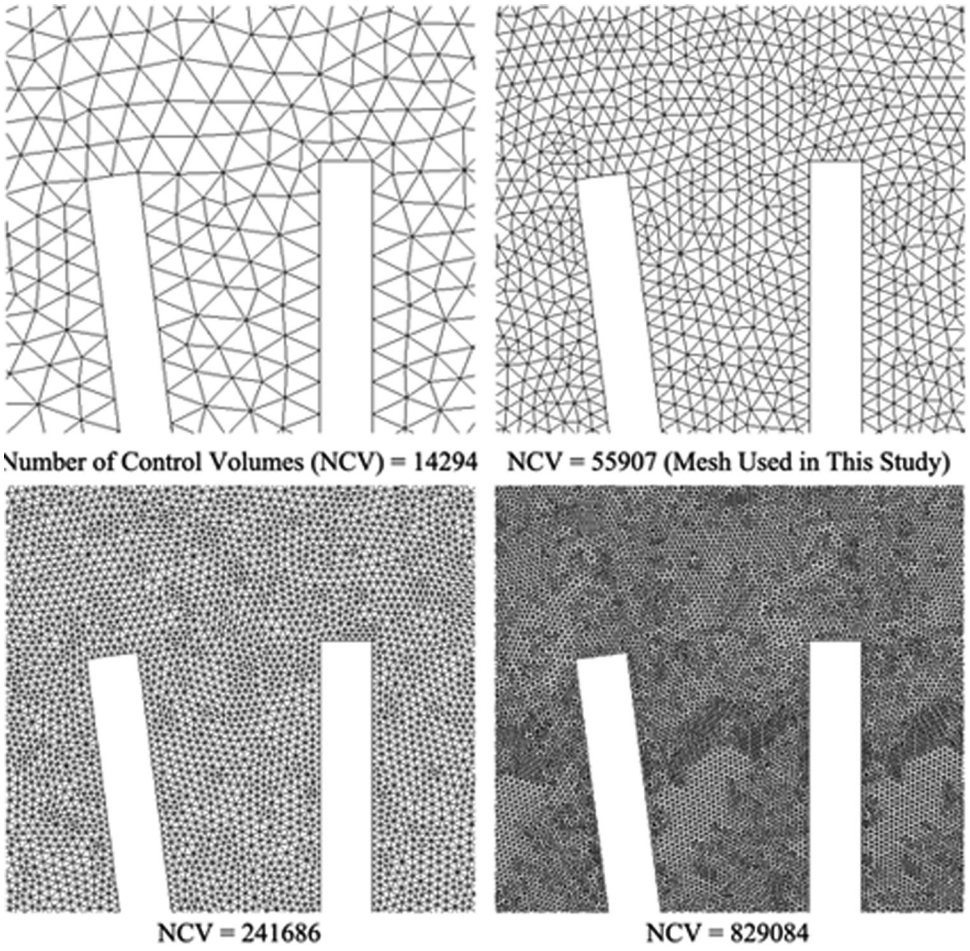

Fig. 5 The meshes used in the grid convergence study

$$q_{r+dr} - q_r = \left(\frac{\mathrm{d}q_r}{\mathrm{d}r}\right)\mathrm{d}r = \mathrm{d}q_f \tag{2}$$

$$dq_r = d\left(-kA\frac{\mathrm{d}T}{\mathrm{d}r}\right) = -k\left(2\pi rt\frac{\mathrm{d}T}{\mathrm{d}r}\right)t\text{: disk thickness}$$

$$\omega(2\pi\mu\rho r^2.\mathrm{d}r) = -2\pi tk\left(\frac{r\mathrm{d}r/\mathrm{d}r}{\mathrm{d}r}\right)\mathrm{d}r \rightarrow T(r) = -\frac{\omega\mu\rho}{9kt}r^3 + C_0\ln(r) + C_1 \tag{3}$$

$$B.C: \text{Insulated at } r_3: \left.\frac{\mathrm{d}T}{\mathrm{d}r}\right|_{r=r_3} = 0 \Rightarrow C_0 = \frac{\omega\mu\rho}{3kt}r_3^3 \tag{4}$$

$$B.C: \text{Outer temperature at } r_2: T(r_2) = T_{\text{out}} \Rightarrow C_1 = T_{\text{out}} + \frac{\omega\mu\rho}{9kt}r_2^3 - \frac{\omega\mu\rho}{3kt}r_3^3\ln(r_2) \tag{5}$$

$T(r)$ in Eq. (3) gives us the temperature field of the disk as a function of r. The Eqs. (4) and (5) present the constants in this

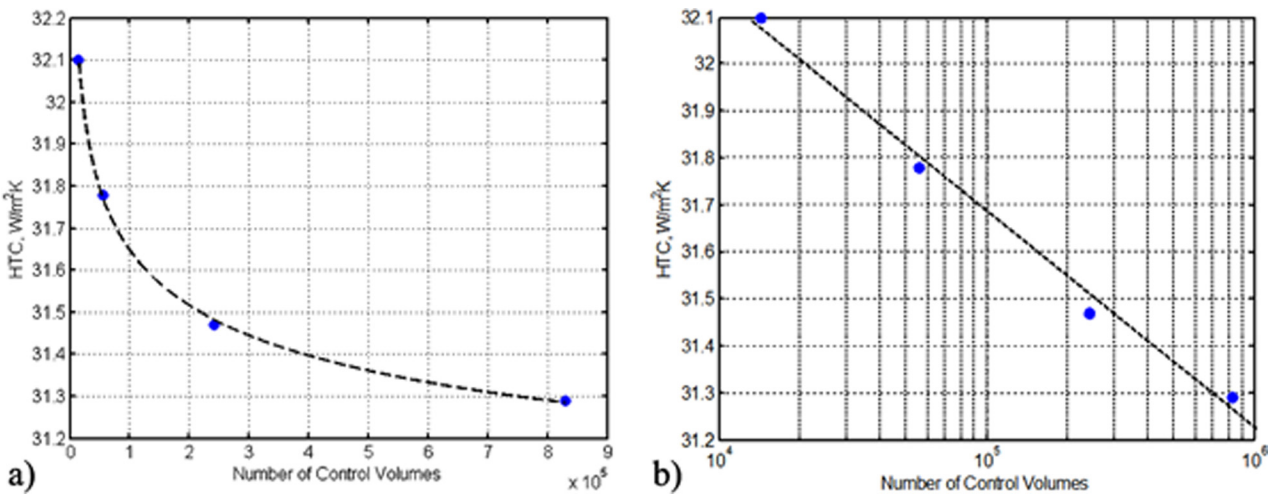

Fig. 6 Investigation of the grid convergence

Downloaded From: http://thermalscienceapplication.asmedigitalcollection.asme.org/pdfaccess.ashx?url=/data/journals/jtsebv/28835/ on 02/06/2017 Terms of Use: http://www.asr

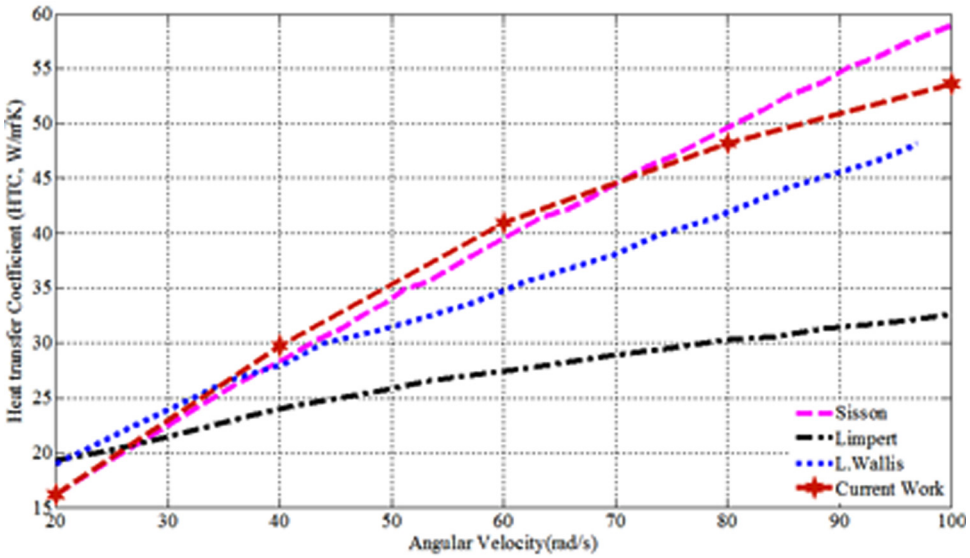

Fig. 7 Comparison of the results of straight vanes disk

equation. Table 1 contains the constants. These constants are for a typical braking system used in ordinary vehicles like sedans [6]. The computing results of this formulation follow the results of studies like Refs. [5,13].

Figure 3 shows the temperature field obtained by this consideration for different angular velocities. As it is clear in the figure, the temperature converges to a maximum magnitude at the largest radius of the disk. This situation is also detected in analytical and experimental research [14,6] where the hotter spots appear earlier in upper surfaces. In this research, the constant critical temperature in the highest radius was assumed as an input for the CFD tool as the working temperature of the vanes for each velocity.

Therefore the aim of this research is to model the vanes of a ventilated brake disk in a steady state approach in which the output result is the average heat transfer coefficient of the vanes. In order to present more tangible results and comparison between the cases, the heat transfer coefficient (HTC) is reported. To compute this parameter the solver simply uses the following formula

$$\mathrm{HTC} = \frac{1}{A} \oiint_s -\frac{k_f \partial T/\partial n}{\Delta T} dA \tag{6}$$

Here k_f refers to the air's thermal conductivity, $\frac{\partial T}{\partial n}$ is temperature gradients normal to the vent's wall, and ΔT is temperature difference between ambient temperature (T_∞) and vent's wall

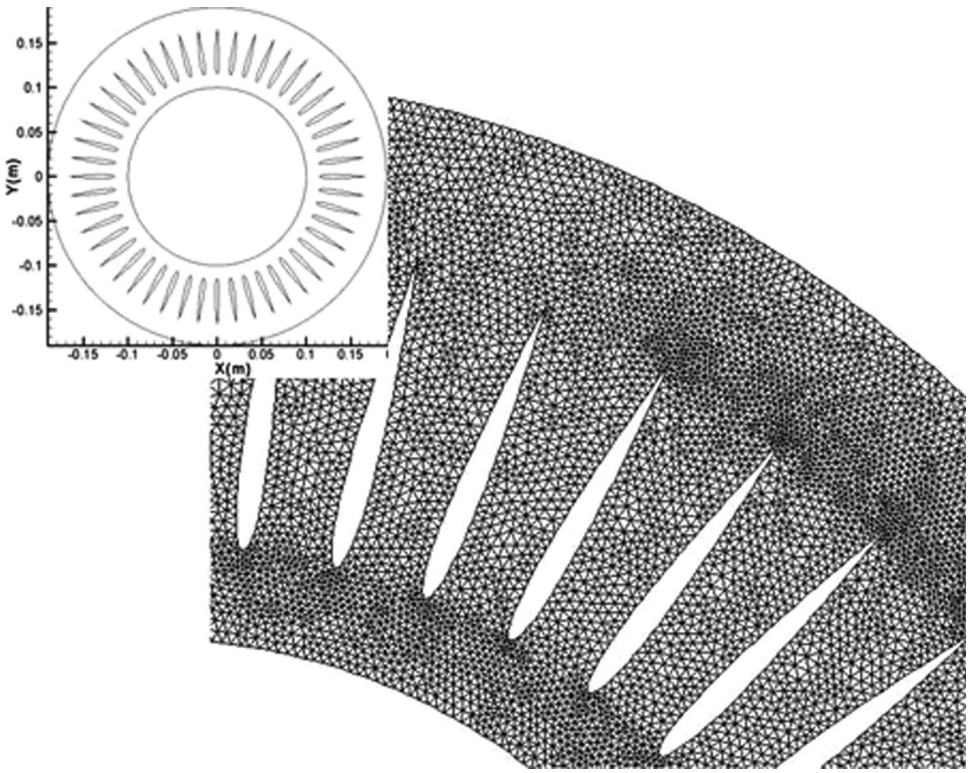

Fig. 8 Ventilation by NACA-0009 (Case1)

Downloaded From: http://thermalscienceapplication.asmedigitalcollection.asme.org/pdfaccess.ashx?url=/data/journals/jtsebv/28835/ on 02/06/2017 Terms of Use: http://www.asr

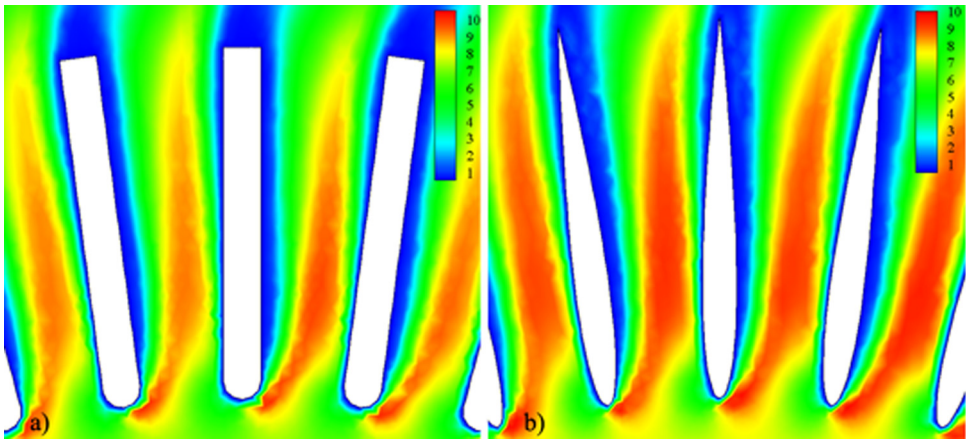

Fig. 9 Contours of velocity magnitude (m/s), (*a*) Straight vanes and (*b*) Case1

temperature. A 2nd-order unstructured finite volume flow solver is used for CFD computation. The realizable k-ϵ turbulence model is used with 4.5% turbulence intensity for the inflow boundary. The flow boundary conditions are set as the pressure boundary both at the inlet and outlet which are the inner and outer hub of the brake disk accordingly. The maximum steady state computed wall temperature (Sec. 2) is 873 K and it is used as the wall boundary condition. The convergence tolerance is set to be 7 orders drop in relative residual for all flow equations. The details of the CFD modeling are presented in Table 2.

2.3 Verification. Each modeling, even the one that considers all interfering parameters, must be compared with some verified research and/or validated experimental results. In this research, the straight vane brake disk is chosen for the verification purpose. Figure 4 shows the meshing used by the CFD tool; the unstructured (triangle) meshing is used for all cases in this study as it can successfully and easily cover the complex geometry curvatures.

Before verifying our CFD computation results, first we perform a grid study case. In order to investigate the solution grid independency and to choose a reasonable mesh resolution, the problem is solved for four different mesh levels at the angular velocity of 40 rad/s. The meshes are shown in Fig. 5 and have 14,294 (M1), 55,907 (M2), 241,686 (M3), and 829,084 (M4) control volumes. The length scale of each mesh is nearly refined by a factor of two resulting in approximate increasing in the mesh size by a factor of four. The computed values of HTC are plotted for all meshes in Fig. 6. The difference between the HTC of M2 and M4 is about 1.6% and this difference reduces to 0.6% for M3 and M4. Considering the trend of grid convergence, scientifically speaking,

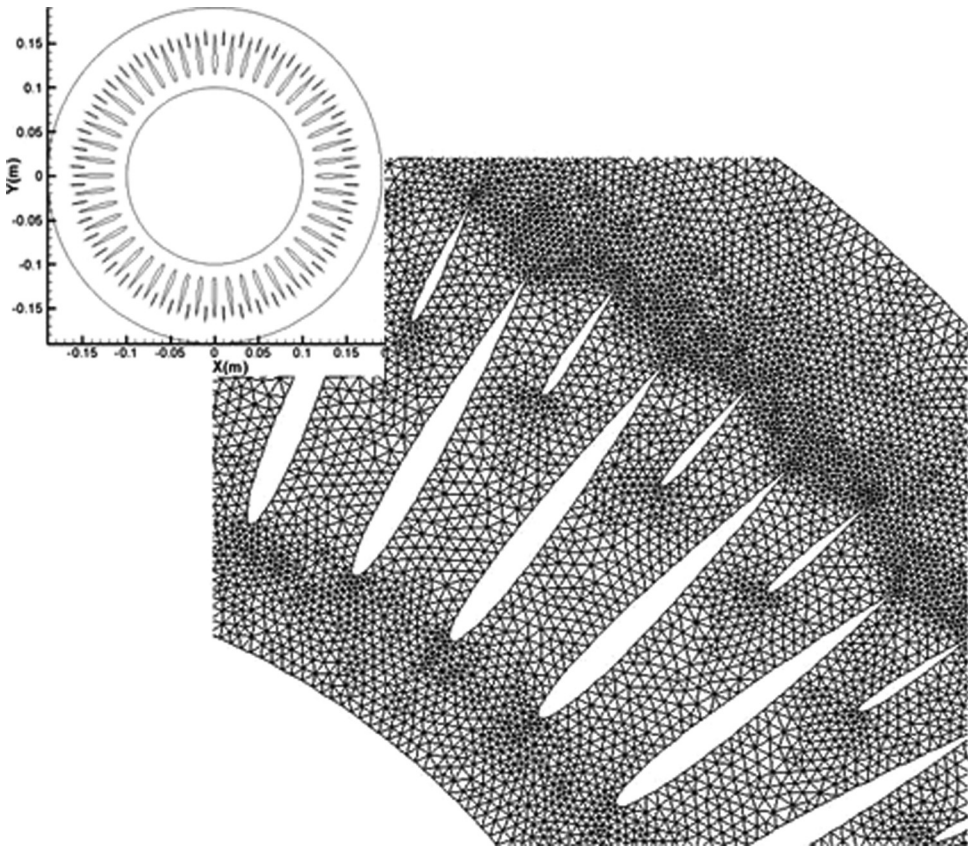

Fig. 10 New design by adding secondary NACA-0009 (Case2)

Downloaded From: http://thermalscienceapplication.asmedigitalcollection.asme.org/pdfaccess.ashx?url=/data/journals/jtsebv/28835/ on 02/06/2017 Terms of Use: http://www.asm

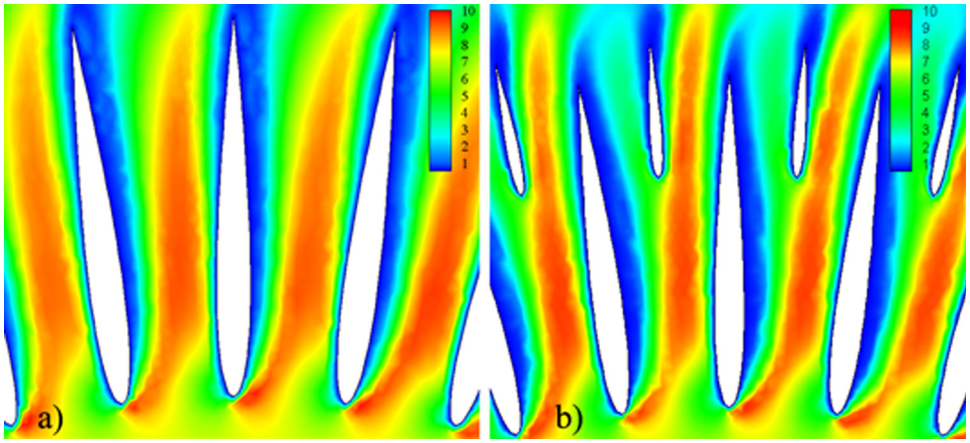

Fig. 11 Contours of velocity magnitude (m/s), (*a*) Case1 and (b) Case2

probably two finer mesh levels are needed for full grid convergence; however, it is safe to say that grid convergence is achieved within reasonable engineering accuracy for the HTC results. Figure 6(*b*) shows that the global mesh refinement in our grid study is performed appropriately since a linear convergence trend for the HTC is obtained in logarithmic scale. The main objective of this research is only to estimate and compare the cooling efficiency of different cooling vanes and the precise computation of the HTC for those configurations are not considered. Therefore the resolution of mesh M2 seems to be reasonably fine enough to estimate the HTC as a design parameter, and this resolution is used for rest of the test cases.

In Fig. 7, the CFD results are compared in different velocities with the results reported in the literature [5–7]; results of the theoretical-empirical correlation model by Sisson [6] differ slightly (7% in the worst case) from the results of the current study. Also, the numerical solution of the Wallis [7] and current study, overall, are in a relatively good agreement. The current CFD computed HTC results have a significant deviation from Limpert [5] results. No judgment can be made here on the accuracy of the results, however, since the geometrical detail of the studied case by Limpert [5] is not exactly the same as our vane geometrical model (as well as other presented studies) some differences between the results are expected.

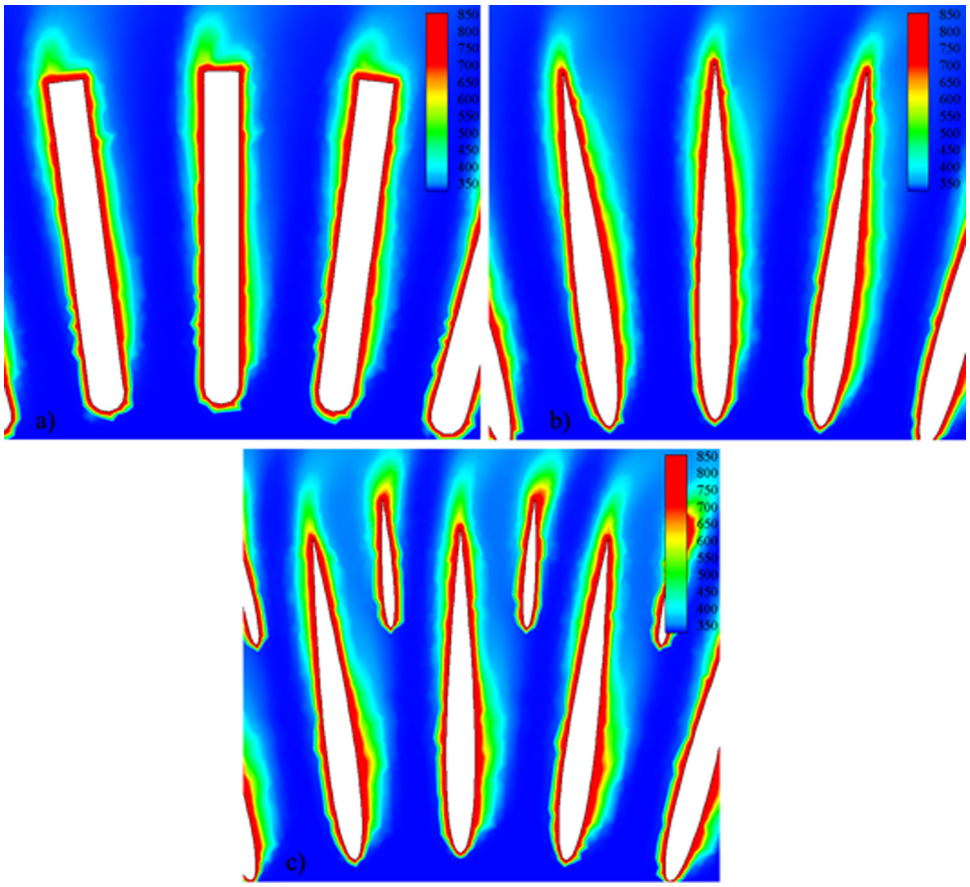

Fig. 12 Contours of temperature distribution (K), (*a*) straight vanes, (*b*) Case1, and (*c*) Case2

Downloaded From: http://thermalscienceapplication.asmedigitalcollection.asme.org/pdfaccess.ashx?url=/data/journals/jtsebv/28835/ on 02/06/2017 Terms of Use: http://www.asm

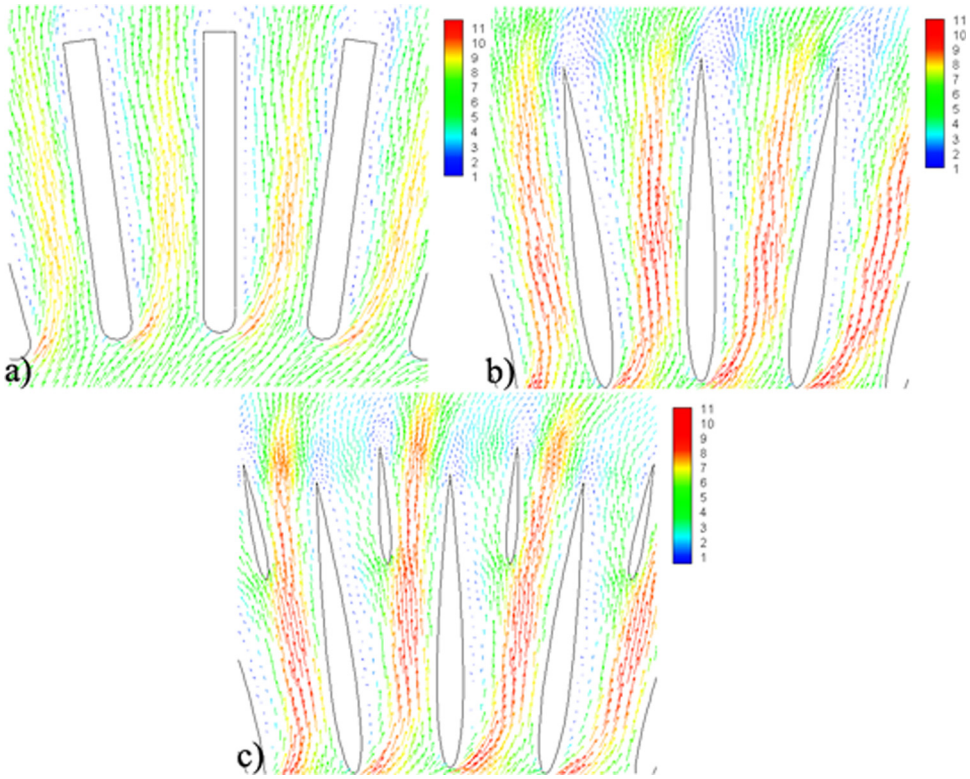

Fig. 13 Vectors of relative *x*, *y* velocity magnitudes (m/s), (*a*) straight vanes, (*b*) Case1, and (*c*) Case2

3 An Improved Novel Geometry

In this section, a new design is presented for ventilating vanes which improves the overall convection heat transfer characteristics significantly.

3.1 Reference Models. Before discussing the new design, a reference model is taken as the base line for comparison. Straight vanes, Fig. 1(*b*), are widely used as the ventilation blades. This simple straight vane configuration was simulated and analyzed in different velocities. Its results are used later on for the comparison purpose.

Recently, many patents are presented by using a special shape of a curved vane (Fig. 1(*b*)) claiming to support an enhanced thermal dissipation. A very new design was presented by Ruiz and Beach [17]. This design makes use of the curved vanes similar to airfoil shapes in its leading edge and combines the properties of a nozzle and diffuser. The studies of these available geometries lead to the following general guidelines toward a new design:

(I) increasing the flow momentum to enhance the heat dissipation which is accomplished by creating a nozzle like geometry
(II) reducing the flow separation region close to the vane leading edge area where the flow has the maximum capacity of heat removal

The first feature (I) is quite helpful since the nozzle increases the airflow velocity between vanes improving the HTC. Higher HTC means the airflow absorbs most of the braking generated heat. The second feature (II) aims at limiting the portion of the vanes that do not noticeably accommodate the cooling process.

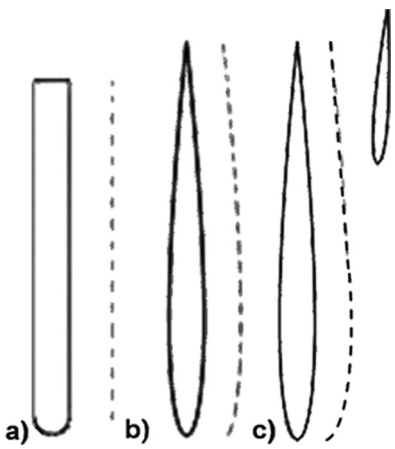

Fig. 14 The zone of the nodes (dashed lines), (*a*) straight vanes, (*b*) Case1, and (*c*) Case2

3.2 Design Strategy. According to the previous discussion, we are motivated to use airfoils for the vane profile of the brake disk. The leading edge curvature of the airfoil rapidly accelerates the flow with minimum pressure drag (as the airfoil is designed for such purpose) making the airfoil a very good candidate to perform the cooling task. The airfoils arrangement creates a suitable passage for the airflow over the brake rotor. The design process is classified into three main steps in which the aim is to increase the thermal efficiency of the disk by the means of the different vane's geometry arrangements. The NACA-0009 profile, due to its superior lift to drag ratio among other NACA airfoil series, is selected as a candidate to explore its performance in the brake disk cooling. In the Case1, the single NACA-0009 is used for the vane's geometry. Figure 8 displays the Case1 geometry and Fig. 9 shows the contours of the velocity magnitude in comparison with straight vanes for radial velocity of 40 rad/s.

Downloaded From: http://thermalscienceapplication.asmedigitalcollection.asme.org/pdfaccess.ashx?url=/data/journals/jtsebv/28835/ on 02/06/2017 Terms of Use: http://www.asm

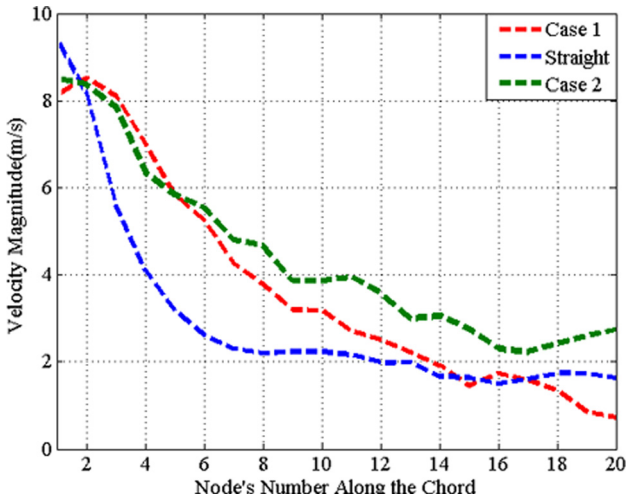

Fig. 15 Comparison of the velocity for selected nodes on the imaginary line

The Fig. 9 clearly explains the effect of the flow acceleration of the new design. The nozzle shapes at the entrance speed up the air to a maximum magnitude but then the air decelerates because it enters the diffusing area. Here the HTC is increased over 6% to 15% in comparison with the straight case for different radial velocities. This is because of the well-positioned nozzle-diffuser shape as well as more tendency of the airflow to stick to the airfoil surface and not to separate from the vane.

Based on the model obtained above, one main flaw in the flow field is obvious and that is the existence of a dead part of the vane which happens to be in backward or in shadow of the neighbor's vane (Fig. 9). To cure this defect partially, a simple solution was adopted in the way depicted in Fig. 10. A secondary NACA-0009 with smaller relative chord is placed close to the end of the brake disk between the passages of the main airfoils in such a way to boost the speed of the airflow again and limits the separation, i.e., the dead region, over the rear part of the brake disk. The result of this new design is demonstrated in Fig. 11 in which the velocity contours of both cases are shown. The effect of added airfoil is obvious due to the considerable reduction of the dead region. To reveal the best quality of this design, in Fig. 12, the contours of temperature are shown. Since the air is accelerated, it has assisted cooling down the vanes especially in areas where the single airfoil design failed to cool down appropriately. Also the regions with high temperature are eliminated in the new design in comparison with straight vanes. The last but not the least is the velocity vector comparison in Fig. 13. This figure uncovers the continued acceleration of the airflow from the primary and secondary airfoils. Also a noticeable reduction in the wake region at the vane trailing edge in comparison with straight model is observed.

As an alternative approach in the detailed analysis of the studied examples, here a line near to the vanes profile (Fig. 14(*a*)–(*c*)) is selected and the velocity of 20 nodes is reported and compared for all test cases. Comparison of the nodes' velocities is shown in Fig. 15. Although some nodes in the Case1 design may experience higher velocities but the overall integral of the velocity for the Case2 design justifies its superior HTC.

To find the proper setting for the secondary airfoils, some test cases including the position and its deviation angle from radial line were performed. Results showed that for ± 5 degrees of deviation from the radial line the overall change in HTC number were lower than 0.1% when compared to the original neutral positioning.

The radial position of the airfoil was also the parameter that could be altered, the small airfoil could be scaled to be placed in $0.4(R_{\text{out}} - R_{\text{in}})$ from the trailing edge of the main airfoil or it is scaled to be at $0.3(R_{\text{out}} - R_{\text{in}})$. These two adjustments had the best result among others. In fact the first had better performance in low speeds and the other in high speeds among other positioning of the airfoil. The high speed and the low speed directly affect the position and the size of low velocity regions where cooling does not happen properly and it lowers the thermal capacity of the vanes. High velocity pushes backward the low speed region therefore small airfoils placed in 0.3 of radial distance is more effective. This phenomena is reversed when it is tested in low velocity and the other geometry $0.4(R_{\text{out}} - R_{\text{in}})$ results in better cooling efficiency.

In all of these design steps, an approach to improve the HTC of the ventilated brake disk was followed by the vanes modification and step by step an improvement in HTC was observed. Table 3 summarizes the test cases and the results that are obtained in this research. The result show an increase of the HTC number of the new vane design up to 17% to 29% for different velocities.

4 Concluding Remarks

A simple approach for modeling of the steady state braking scenario was presented. The verification of the numerical simulation of such braking scenario for the heat transfer coefficient, HTC, of the straight vanes was conducted against both theoretical-empirical data as well as another numerical simulation. The flow fields of the various air passage topologies were modeled via CFD simulation. Some detailed analysis was performed by studying the velocity and temperature distribution around vanes. The result showed that the increasing the flow momentum and limiting the flow separation region especially close to the leading edge of the vanes are the key factors in overall HTC improvement. A novel design was introduced by means of two airfoils as primary and secondary vanes improving the air pumping efficiency noticeably. The overall HTC was enhanced 17% to 29% for different angular velocities using the new design. It is worth mentioning that the manufacturability and the final price of such a product, i.e., a brake disk with airfoil vanes, need to be investigated separately, and is beyond the scope of current study. As a future work we intend to optimize the gap size between vanes, the location and the shape of the secondary vane to achieve the optimal HTC for a double vane disk brake.

Table 3 Summary of the results

Average vent heat transfer coefficient (W/m^2 K)	Geometries		Disk's angular velocity (rad/s) 20	40	60	80	100
	Straight vanes		18.16	31.78	43.02	50.18	53.66
	Airfoil vanes	Case1 (Fig. 3)	19.71	34.284	45.81	55.74	61.91
		HTC improvement[a]	**8.54%**	**7.88%**	**6.49%**	**11.08%**	**15.38%**
		Case2 (Fig. 5)	23.505	39.76	50.57	59.06	66.09
		HTC Improvement[a]	**29.43%**	**25.12%**	**17.55%**	**17.71%**	**23.15%**

[a]Improvements are calculated in comparison with the straight vane case.

Downloaded From: http://thermalscienceapplication.asmedigitalcollection.asme.org/pdfaccess.ashx?url=/data/journals/jtsebv/28835/ on 02/06/2017 Terms of Use: http://www.asr

References

[1] Lee, K., 1999, "Numerical Prediction of Brake Fluid Temperature Rise During Braking and Heat Soaking," SAE Paper No. 01-0483.

[2] Valvano, T., and Lee, K., 2000, "An Analytical Method to Predict Thermal Distortion of a Brake Rotor," SAE Paper No. 01-0445.

[3] Orthwein, W. C., 2004, *Clutches and Brakes Design and Selection*, 2nd ed., Marcel Dekker, New York.

[4] Limpert, R., 1999, *Brake Design and Safety*, 2nd ed., SAE International, Warrendale, PA.

[5] Limpert, R., 1975, "Cooling Analysis of Disk Brake Rotors," SAE Paper No. 751014.

[6] Sisson, A. E., 1978, "Thermal Analysis of Vented Brake Rotors," SAE Paper No. 780352.

[7] Wallis, L., Leonardi, E., Milton, B., and Joseph, P., 2002, "Air Flow and Heat Transfer in Ventilated Disk Brake Rotors With Diamond and Tear-Drop Pillars," Numer. Heat Transfer Part A, **41**, pp. 643–655.

[8] Gao, C. H., and Lin, X. Z., 2002, "Transient Temperature Field Analysis of a Brake in a Non-Axisymmetric Three-Dimensional Model," J. Mater. Process. Technol., **129**, pp. 513–517.

[9] Johnson, D. A., Sperandei, B. A., and Gilbert, R., 2003, "Analysis of the Flow Through a Vented Automotive Brake Rotor," J. Fluids Eng., **125**, pp. 979–987.

[10] Sakamoto, H., 2004, "Heat Convection and Design of Brake Disks," Inst. Mech. Eng., **218**(3), pp. 203–212.

[11] Chi, Z., Naterer, G., and He, Y., 2008, "Effects of Brake Disk Geometrical Parameters and Configurations on Automotive Braking Thermal Performance," CSME Trans., **32**(2), pp. 313–324.

[12] Mcphee, A. D., and Johnson, D. A., 2008, "Experimental Heat Transfer and Flow Analysis of a Vented Brake Rotor," Int. J. Therm. Sci., **47**, pp. 458–467.

[13] Talati, F., and Jalalifar, S., 2008, "Investigation of Heat Transfer Phenomena in a Ventilated Disk Brake Rotor With Straight Radial Rounded Vanes," J. Appl. Sci., **8**(20), pp. 3583–3592.

[14] Talati, F., and Jalalifar, S., 2009, "Analysis of Heat Conduction in a Disk Brake System," Heat Mass Transfer, **45**, pp. 1047–1059.

[15] Incropera, F. P., and Dewitt, D. P., 1996, *Fundamentals of Head and Mass Transfer*, 4th ed., Wiley, Toronto, Canada.

[16] Yano, M., and Murata, M., 1993, "Heat Flow on Disk Brakes," SAE Paper No. 931084.

[17] Ruiz, S. J., and Beach, R., 2004, "Ventilated Brake Rotor," US Patent No. 6,796,405 B2.

Downloaded From: http://thermalscienceapplication.asmedigitalcollection.asme.org/pdfaccess.ashx?url=/data/journals/jtsebv/28835/ on 02/06/2017 Terms of Use: http://www.asr